© 2015 IJSRSET | Volume 1 | Issue 4 | Print ISSN : 2395-1990 | Online ISSN : 2394-4099
Themed Section: Science and Technology

Temporal Monitoring of SAR Polarimetric Parameters and Scattering Mechanism for Major Kharif Crops and Surrounding Land Use

Bindi P. Shastri[1], Dipanwita Haldar[2], Shiv Mohan[3]
[1]Faculty of Technology, CEPT University, Ahmedabad, Gujarat, India
[2]Advanced Techniques Development Group (ATDG), Space Applications Centre, ISRO, Ahmedabad, Gujarat, India
[3]PLANEX/ Physical Research Laboratory, Ahmedabad, Gujarat, India

ABSTRACT

Spatial and temporal monitoring of agricultural crop is one of the important aspects for the agricultural production estimation for India. Among the various remote sensing tools, role of polarimetric SAR is being evaluated for the assessment of its utility in providing improved information. In view of importance of polarimetric techniques, it is necessary to understand the role of polarimetric indices and decomposition techniques for improved identification and discrimination of different land cover classes. An attempt has been made to study temporal changes in polarimetric parameters and decomposition algorithm for monitoring landuse classes dominated by agricultural land using full polarimetric C-band radarsat-2 data set. Various polarimetric parameters like Radar Vegetation Index, polarimetric decomposition techniques like Freeman Durden, and Pauli Decomposition have been used to evaluate the capability of multi polarimetric and multi temporal SAR for landuse identification, discrimination and classification. Along with the above work, sub classification of RVI values and scattering behavior of the major Kharif crops and other land targets has been done. Temporal change in mean RVI value from 0.48 to 0.66 allowed to demarcate the aerial extent of agriculture/ vegetation cover. Based on the crop growth cycle during Kharif season, a very clear change in RVI value range from 0.4-0.6to 0.8-1.5 was noticed during crop growth. Cotton, Paddy and Gwar could be well discriminated based on change in RVI values with respect to their growth cycle. Freeman Durden Decomposition was found to have overall higher classification accuracy of 95%, followed by Pauli Decomposition (90%) and RVI parameter (49%). Temporally, in all cases, highest classification accuracy was obtained for three date data of July, August and September months.

Keywords: Backscattering, Radar Vegetation Index, Polarimetric parameters, Decomposition Techniques, Classification

I. INTRODUCTION

Radar Polarimetry is renowned for its application in extraction of constructive information from data in order to distinguish various targets. Fully polarimetric data due to conservation of all polarimetric information plays an important role in describing physical information about the target like shape, orientation, symmetry, non-symmetry or irregularity of the target. The polarimetric information contained in polarimetric SAR images represents the great potential for the characterization of natural and urban surfaces. The polarimetric indices or parameters are polarimetric SAR observables extracted from polarimetric data which have some physical meanings associated with them that describe the scattering behavior of the target [11].

Synthetic Aperture Radar (SAR) sensors that acquire imagery at a single transmit-receive polarization provide one-dimensional datasets. Consequently, multi-date imagery is usually required to provide meaningful information on crops. Research has demonstrated that additional polarizations will increase the information content in a SAR dataset. The importance of SAR Polarimetry in crop classification/identification arises principally because polarization is sensitive to vegetation orientation. Hence, it provides a means to distinguish crops with different canopy architectures as

well as growth stages. Polarization dependent indices of which represent scattering mechanisms such as attenuation due to vegetation and depolarization due to vegetation scattering can be studied for target responses. Type of vegetation, density and architecture of canopy materials control the behavior of polarimetric channels. The canopy constituents make the target medium randomly oriented as the plants grow and can be studied considering volume scattering components and parameters based on the same [10].

Synthetic Aperture Radar (SAR) data has shown promising results in crop discrimination and classification with reasonably high accuracy. Traditionally, crop classifications are done using multi-date SAR data that uses phenological information of crops to discriminate them. Single-date multi-polarization SAR data also has the potential to identify crops based on the variation in their scattering signatures in different polarizations. Various authors have reported of achieving significant classification accuracies for crops and other landuse classes using dual and quad polarimetric data from airborne as well as space borne SARs [1].

A radar vegetation index (RVI) proposed by Kim and Van Zyl, 2001 [9] was used to develop cut-off values to separate cropped areas from non-vegetated area. Moreover, an attempt has been made to discriminate various crops and other land uses based on these RVI values. SAR Decomposition techniques like Freeman Durden and Pauli decomposition were also used to discriminate the major Kharif crops with respect to their temporal growth cycle along with other landuse classes like urban, water body etc., in order to observe change in scattering mechanisms.

This paper aims to study and evaluate role of polarimetric indices and decomposition techniques for identification and discrimination of different land cover classes by using fully polarimetric C-band Radarsat-2 data. Various polarimetric parameters like Radar Vegetation Index, polarimetric decomposition techniques like Freeman Durden, and Pauli Decomposition have been used the evaluate the capability of polSAR for landuse identification and classification.

Study Area and Experimental Data

Central State Farm located in Hisar district of Haryana (India) has been selected for the present study. The area lies between the coordinates 29° 11′ - 29° 20′ N latitudes and 75° 36′-75° 45′E longitudes. The study area, with a size of more than 5 hectares, majorly comprises of agricultural farmland, surrounded by fallow and scrub lands, few village clusters and small water bodies (ponds). The major crops grown here during *Kharif* (summer/monsoon) season are Cotton, Paddy, Gwar and other pulses, while those grown in *Rabi* (winter) season include Wheat, Gram, Mustard and Pea. This site was selected for developing a methodology for land use discrimination polarimetric SAR data. Polarimetric SAR data were acquired on different dates over crop calendars. Synchronous ground truth information including vegetation and soil parameters viz. sowing date, crop stage, method of sowing, row-spacing for row crops, plant density, plant height, leaf area, crop vigor, expected date of harvest, background soil, soil type, soil moisture, field size etc. corresponding to the date of acquisitions of all the SAR data were collected for subsequent analysis [4].

Table I. Details of Radarsat-2 Data used in this Study

Sr. No.	Polarization	Central Inc. Angle	Acquisition Mode and beam	Ground Range Pixel spacing	Date of Acquisition: dd/mm/yyyy
1	Full: HH,HV, VH,VV	40°	Descending, right looking FQ21	6m	29/06/2011
2	-do-	-do-	-do-	-do-	23/07/2011
3	-do-	-do-	-do-	-do-	16/08/2011
4	-do-	-do-	-do-	-do-	9/09/2011
5	-do-	-do-	-do-	-do-	3/10/2011

Fully Polarimetric, Quadpol (HH, HV, VH, VV), C-band Radarsat-2 data, dated 29th June, 23rd July, 16th August, 9th Sept and 3rd October 2011, has been used to conduct this study along with ground truth information. The Radarsat-2 data was acquired as SLC (Single Look Complex) data, with descending right looking FQ21 acquisition beam mode, 40° Central incidence angle, and with 6m ground range pixel spacing. In SLC data, each resolution cell of the image, called pixel is characterized by amplitude value (represents the strength of the returned signal) and an absolute phase value (represents the time delay of the received signal in a coherent system), both are jointly represented as a ‘complex

number'. Details of all the datasets used have been given in table 1.

II. METHODS AND MATERIAL

For obtaining results to the current study, the methodology was broadly divided into two parts, based on backscattering coefficient values of various land uses, followed by the generation of polarimetric parameters like Radar Vegetation Index, Span etc. Here the SLC data from quadpol C-band Radarsat-2 data was extracted for five months namely June, July, August, September and October, using. This was followed by generation of multilook images, its geocoding and layer stacking for all the five quadpol datasets. Speckle suppression using Lee 3x3 filter was done, followed by generation of backscatter coefficient images (dB). These fully polarimetric multi-temporal datasets were then visualized and analyzed (based on backscattering value) for identification of various crops and surrounding land use, along with ground truth information to support the results. In the second case, Coherency (T3) matrix was generated for all the five datasets, followed by its geocoding. Based on the geocoded T3 matrix, Freeman Durden Decomposition and Pauli Decomposition was performed for all the datasets. These image results were then resized and registered to that of the backscatter images for further analysis, interpretation, followed by their supervised classification. ENVI and PolSARpro softwares have been used during the study.

A. Radar Vegetation Index

RVI based on cross-polarization and total power ratio not only shows higher sensitivity to biomass but also characterized biomass over hill slopes where single polarization signals had limitation due to slope induced variation in radiometry of SAR signal [11].

A comparative study between RVI and NDVI of Landsat TM data was done by F.Ling et. al. (2009) for forest area mapping. After examining of the index maps and the corresponding histograms, forest/ non-forest segmentation was performed by unsupervised classification and by threshold method. The results show that RVI is much better in this kind of application [14].

Polarized radar signal is sensitive to the scattering types. It is observed that for surface scattering conditions $|S_{vv}|^2 > |S_{hh}|^2$, for double-bounce scattering conditions $|S_{vv}|^2 > |S_{hh}|^2$, and for vegetation or volume scattering conditions $|S_{vv}|^2 > |S_{hh}|^2$ and

These conditions may lead to formulate an index for vegetation called radar vegetation index (RVI) which can be denoted as:

$$RVI = \frac{8|S_{hv}|^2}{|S_{hh}|^2 + |S_{vv}|^2 + 2|S_{hv}|^2} \quad (1)$$

This parameter helps in separating vegetation from non-vegetated area in a radar image. RVI value greater than '1' indicates vegetation scattering. RVI in L-band SAR has been found to have good correlation with forest biomass [9].

B. Polarimetric Decomposition Techniques

Freeman Durden Decomposition: The Freeman-Durden approach is based on the decomposition of power reflection matrix of a scatterer. The scattering mechanism of a target or an ensemble of targets can be explained through a 3x3 scattering matrix (the coherency [T] or the covariance [C] matrix) in power domain for monostatic case. The Freeman-Durden decomposition models the covariance matrix as the contribution of three scattering mechanisms (Freeman et. al. 1998; Lee et. al. 2004): (1) Volume scattering where a canopy scatterer is modeled as a set of randomly oriented dipoles, (2) Double-bounce scattering modeled by a dihedral corner reflector and (3) Surface or single bounce scattering modelled by a first-order Bragg surface scatterer.

$$[C] = f_s[C_{surface}] + f_d[C_{double}] + f_v[C_{volume}] \quad (2)$$

Where, the terms fv, fd and fs correspond to the contribution of the volume scattering, double-bounce scattering and surface-like scattering, respectively to the final covariance matrix [C].

According to this model, the measured power P may be decomposed into three quantities:

$$P = P_{surface} + P_{double-bounce} + P_{volume} \quad (3)$$

Where,

$$P_s = f_s\left(1+|\beta|^2\right),\ P_d = f_d\left(1+|\alpha|^2\right),\ P_v = 8f_v/3$$

Consequently, the scattered power Pv, Pd and Ps were employed to generate a RGB image to present all the color-coded polarimetric information in a sole image.

Assumptions:

-Like-polarized and cross-polarized elements are uncorrelated:

$$\left\langle S_{hh}S_{hv}^{*}\right\rangle \approx \left\langle S_{vv}S_{hv}^{*}\right\rangle \approx 0$$

-The cross-polarized response is generated by the volume scatterer only.

This method is based on simple physical scattering mechanism (surface scattering, double bounce scattering, and volume scattering). The contribution of each of the three scattering mechanisms to the total power are shown for each pixel usually with surface scattering as red, volume scattering as green, and double bounce scattering as blue [6] [13].

C. Pauli Decomposition

Instead of the matrix notation, a four element complex vector $\vec{k}$ may be used to explain a target scattering, which contains complete information on the [*S*] matrix.

$$[S]=\begin{bmatrix} S_{hh} & S_{hv} \\ S_{vh} & S_{vv} \end{bmatrix} \Rightarrow \vec{k}=\frac{1}{2}Trace([S]\Psi)=[k_0,k_1,k_2,k_3]^{T} \quad (4)$$

Where '†' denotes the vector transpose, Trace ([S]) is the sum of the diagonal elements of matrix [S] and ψ are a set of 2x2 complex basis matrices, which are constructed as an orthonormal set under a hermitian inner product (i.e., their eigenvalues are real and non-negative and their eigenvectors are orthogonal). A basis, which is more related to the physics of wave scattering, the Pauli basis, is formed by the Pauli spin matrices [2] [3] [13].

$$\Psi_P=\left\{\sqrt{2}\begin{bmatrix}1&0\\0&1\end{bmatrix},\sqrt{2}\begin{bmatrix}1&0\\0&-1\end{bmatrix},\sqrt{2}\begin{bmatrix}0&1\\1&0\end{bmatrix},\sqrt{2}\begin{bmatrix}0&-i\\i&0\end{bmatrix}\right\}$$

The corresponding vector $\vec{k}$p then becomes:

$$\vec{k}_P=\frac{1}{\sqrt{2}}[S_{hh}+S_{vv},S_{hh}-S_{vv},S_{hv}+S_{vh},i(S_{vh}-S_{hv})]^{T}$$

The Pauli decomposition approach assigns the appropriate deterministic scattering mechanisms to each one of the four elementary scattering matrices. The first three components of the above vector are usually interpreted in terms of a sphere, an un-rotated dihedral and a dihedral rotated 45° about the line-of-sight, respectively (Table 2). The fourth component is a cross-polarizer term, which is non-existent for the backscattering. The 'Shv+Svh' term is sometimes associated with "diffuse scattering" or "volume scattering" in connection with incoherent scattering formulations. However, it appears that such interpretations are heuristic and only partly account for the actual phenomena.

Using the Pauli decomposition an RGB image (Pauli image) can be constructed with the 'odd bounce', 'even bounce', and '45◦ tilted even bounce' components in red, blue and green colours, respectively representing all the polarimetric information of matrix [S] [13].

Table II. Pauli Matrices and their interpretation in the ($\vec{E}_h$, $\vec{E}_v$) polarization basis

Pauli Matrix	Pauli Elements	Scattering type	Interpretation
$\begin{bmatrix}1&0\\0&1\end{bmatrix}$	$\frac{S_{hh}+S_{vv}}{\sqrt{2}}$	Odd Bounce	Surface, sphere, trihedral corner reflectors
$\begin{bmatrix}1&0\\0&-1\end{bmatrix}$	$\frac{S_{hh}-S_{vv}}{\sqrt{2}}$	Even Bounce	Dihedral
$\begin{bmatrix}0&1\\1&0\end{bmatrix}$	$\sqrt{2S_{hv}}$	Even Bounce 45° tilted	45° tilted dihedral
$\begin{bmatrix}1&-i\\-i&1\end{bmatrix}$	$\frac{[i(S]_{hh}-S_{vv})}{\sqrt{2}}$	Cross Polarizer	Not existent for backscattering

III. RESULTS AND DISCUSSION

A. Temporal Study of Radar Vegetation Index (RVI)

Radar Vegetation Index was retrieved for C-band Quadpol Radarsat-2 data, of Haryana State Farm and surrounding areas, from June to October respectively. Temporally as well as spatially, a very clear change in the RVI pattern was observed in the study area from June to October. Temporally, it could observed that the amount of green classified areas (RVI range from 0.2-0.4, in figure no. 1), where fallow areas existed,

increased greatly from June to July. With the onset of August month, major areas got converted to magenta (0.8-1.5), followed by blue (0.4-0.6) and yellow (0.6-0.8) classes respectively [11]. This change is due to initial growth of Kharif crops, inside the state farm boundary (cotton, gwar, etc.) as well as on the outside (majorly paddy). Further intensification of the RVI values in a similar manner was observed in September, by the time where the crops are in their maturity stage. By the month of October the crops are totally matured and ready to harvest [10]. Hence, again the onset of green class (0.2-0.4) begins to show. Figure 2 and table 3 shows the change in RVI values of Cotton, Paddy, Gwar, Fallow, Urban and water areas from June to October. Based on the ground truth, AOI of RVI values of major Kharif crops and surrounding landuse was extracted. Water and Urban were observed to have low RVI values, being less than 0.2. In case of urban, no changes were observed as the scattering mechanism did not change with time. However in case of water, the growth of algae and other water plants during August and September, did show a slight increase in the RVI value, thus showing the effect of vegetation growth on scattering change. In case of the crops, based on the growth cycle of each crop, a change in the RVI values was observed from June to October months. In all cases it was seen that highest RVI values were observed when the crop was fully mature and ready to harvest (September, October). While during the sowing or initial growth stage, low RVI values were observed (June July). However not much work at sub classification level of land targets with respect to RVI was found.

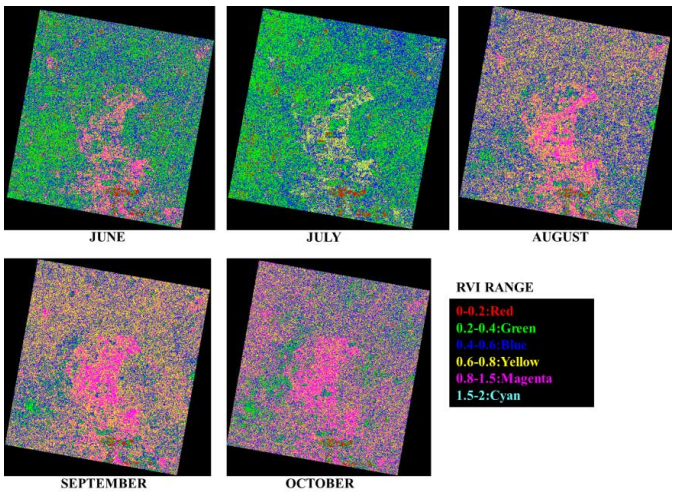

Fig. 1. Temporal Change in Radar Vegetation Index

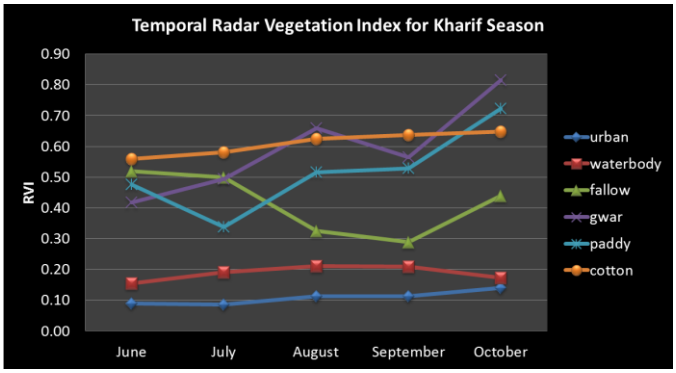

Fig. 2. Temporal Change in RVI of various crops and other landuse classes

Table III. Temporal change in RVI values of various landuse classes

	Urban	Water	Fallow	Gwar	Paddy	Cotton
June	0.09	0.16	0.52	0.42	0.48	0.56
July	0.09	0.19	0.50	0.49	0.34	0.58
Aug	0.11	0.21	0.33	0.66	0.52	0.62
Sept	0.11	0.21	0.29	0.57	0.53	0.64
Oct	0.14	0.17	0.44	0.81	0.72	0.65

B. Temporal Change in Scattering Behaviour using Decomposition Algorithms

Freeman Durden Decomposition:

With the help of Freeman Durden Decomposition of the fully polarimetric quadpol data, the change scattering mechanism of major Kharif crops and surrounding landuse could be observed over time. Figure no. 3 shows the change of study area in terms of its scattering mechanism, namely double bounce, volume and surface scattering. All the urban areas contributed to double bounce scattering, with little to no change in its intensity, as the settlement areas remained steady overtime. It is a characteristic scattering modelled by dihedral corner reflectors like buildings and other built features. Fallow areas, water bodies, and smooth surfaces like bare grounds and roads contributed to surface scattering. The contribution from surface scattering was found to greatly decrease and convert to volume scattering, from June to July, August September and October, wherein the contribution from the former scattering type again started increasing, with the crop harvest, leaving the fields bare again [10]. This change in scattering behavior was observed as the empty fields in June, started having the crop growth with the onset of Kharif Season, up till fully matured and ready to harvest by October (Figure 4). Due to the increased roughness,

as a result of crop growth, the surface scattering got converted to volume scattering over time. In general, surface scattering occurs at the air soil interface. For a perfectly smooth surface, the incident wave will excite the atomic oscillators in the dielectric medium at a relative phase such that the re-radiated field consists of two plane waves, i.e. reflected wave, refracted wave and transmitted wave. For a rough surface, energy is equally distributed in all the directions, which is dependent upon the roughness of the surface and dielectric properties of the surface [6] [13].

Figure 5 shows the temporal change in intensity of surface, volume and double bounce scattering for various land use classes like cotton, paddy, gwar, fallow, water and urban areas respectively. In case of double bounce scattering, urban targets contributed greatly to the same in all the seasons, followed by crops (due to height changes) and least by water body. In case of volume and surface scattering, a change in intensity of both could be observed over all the months, and with advance in the crop growth cycle. Then volume scattering components was maximum in the months of August and September, when the crops were fully grown. In August, Cotton contributed maximally (full growth phase) to the scattering intensity, followed by gwar, paddy, fallow and water body. In September maximum scattering intensity was from Gwar, fallow, paddy followed by cotton and water body. This showed that the other crops apart from cotton matured fully in September. In October, with the onset of harvesting season, the volume scattering component decreased in all the features, with an increased contribution from surface scattering. This change in scattering can be observed from the surface scattering plot of all the features.

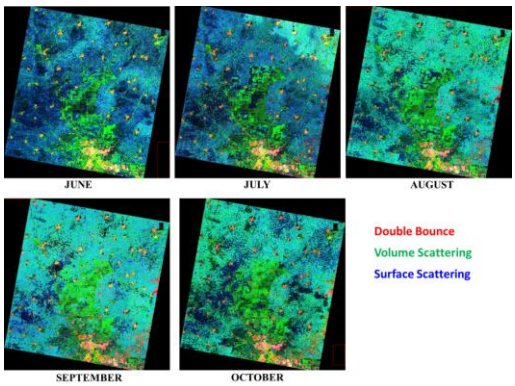

Fig. 3. Temporal Change in Scattering Behaviour – Freeman Durden Decomposition

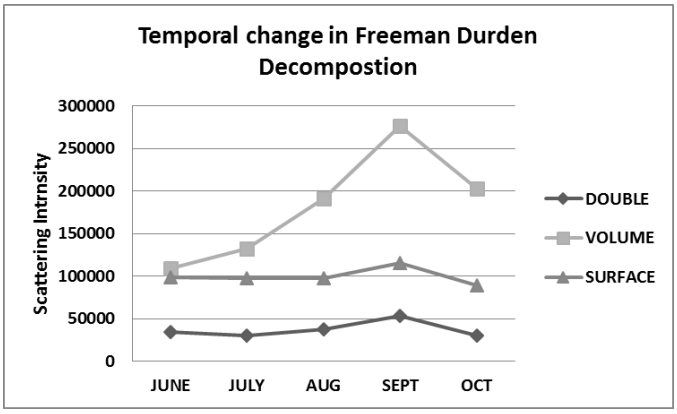

Fig. 4. Temporal Change in Double bounce, Volume, and Surface scattering parameters.

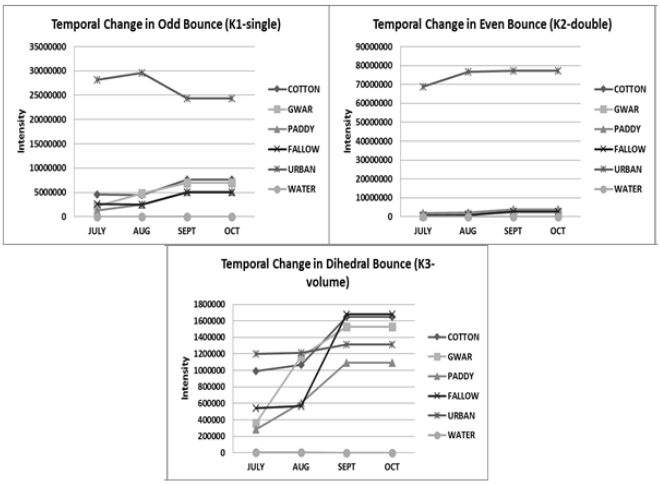

Fig. 5. Temporal change and Response of scattering behaviour of various land use classes in Double bounce, Volume and Surface scattering

Pauli Decomposition

Pauli Decomposition was also performed to observe changes in the scattering mechanism of various land features temporally (Figure 6), as done in case of Freeman Durden Decomposition. When evaluating the results of this analysis, it was found to discriminate land features more effectively than figure 5, especially in case of temporal change in intensity of dihedral bounce scattering for various land use classes like cotton, paddy, gwar, fallow and water respectively. While homogenous features like urban settlements, in comparison to former were clearly demarcated using Pauli Decomposition than in case of Freeman Durden Decomposition. In case of odd bounce scattering (K1, surface scattering), a very clear progressive increase in its intensity was observed was all crops from July to October, with water an urban remaining nearly constant. While K2 parameter (double bounce effect, even bounce) clearly demarcated high

urban scattering from rest of the features. In case of Dihedral bounce/volume scattering, a very clear increase in the intensity rise of the same was observed till September, with a constant value in October thereafter [13]. From the temporal analysis of this decomposition, a very clear crop growth was observed from August to September in all crops, with changing intensity of the same from July to August, depending on the date of sowing of each crop type (figure 8).

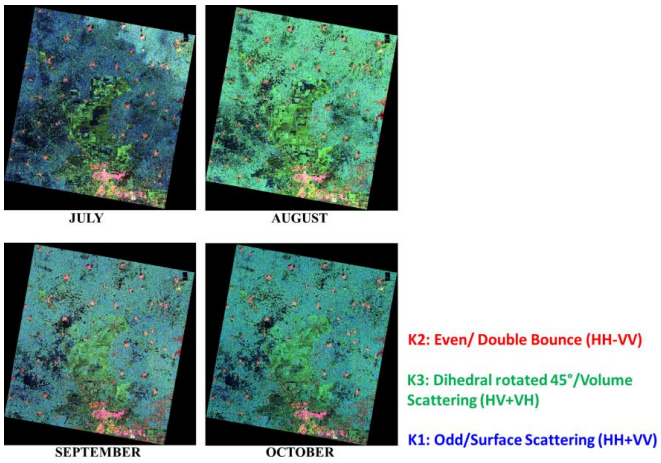

Fig. 6. Temporal Change in Scattering Behaviour – Pauli Decomposition

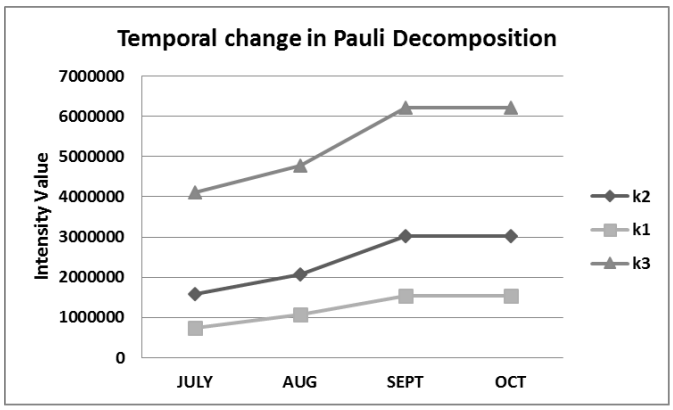

Fig.7. Temporal change in Odd bounce (K1), Even Bounce (K2) and dihedral rotated 45◦ (K3) parameters

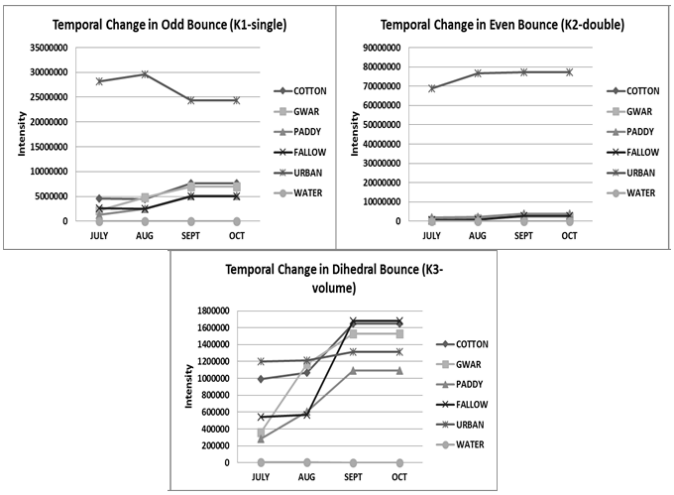

Fig.8. Temporal change and Response of scattering behaviour of various land use in Odd bounce (K1), Even Bounce (K2) and dihedral rotated 45◦ (K3) parameters

Evaluation of classification Accuracy for Landuse using Polarimetric SAR data

The results obtained from the RVI analysis and polarimetric decomposition theorems, were then classified using various data combinations, via Maximum Likelihood classification. From the overall accuracy obtained in each case, three date Freeman Durden Decomposition (July, August, and September), and Pauli Decomposition (July, August, and September) were more accurate as compared to three date RVI classification, with the values being 95%, 90.1% and 49.1% respectively [11].

Two date volume scattering component of Freeman Durden, Pauli Decomposition and RVI were combined with HH backscatter component. In this case, an improvement in overall classification accuracy was seen in HH and RVI combination (73.3%), than the two date RVI analysis (61%) [12]. Similarly HH and volume component of Freeman Durden gave better classification accuracy as compared to two date Freeman Durden Decomposition Analysis. In all the classification combinations, the overall classification accuracy increased in case of two date July-August combination, and three date July-August-September combination. Hence showing the effect of change in scattering mechanism of various land targets over a given time period. The classification outputs are as shown in figure no.9 and the accuracy values have been shown in table 3.

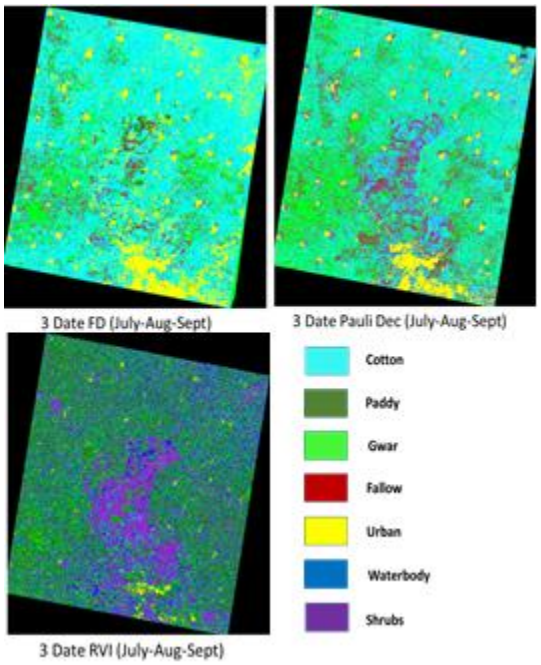

Fig.9. Supervised Maximum Likelihood using three date combination of Freeman Durden Decomposition, Pauli Decomposition and RVI Analysis

Table IV. Feature wise and Overall Classification Accuracy for polSAR parameters

CLASSIFICATION ACCURACY (%)									
	Cotton	Paddy	Gwar	Fallow	Shrubs & Plantation	Urban	Waterbody	Overall Accuracy	Kappa Coefficient
RVI (June-July)	4.0	77.0	25.0	15.0	24.0	92.2	60.8	39.2	0.3
RVI (July-August)	29.8	84.7	70.2	46.0	92.0	91.7	86.2	61.0	0.5
RVI (August-Sept)	0.1	70.6	51.8	13.5	68.0	94.6	85.7	40.4	0.3
RVI (Sept-Oct)	7.9	44.7	28.7	24.3	46.0	91.7	70.6	39.9	0.3
RVI (June-July-August)	14.7	84.7	46.8	20.3	60.0	92.2	74.5	47.8	0.4
RVI (July-August-Sept)	12.4	78.8	51.1	25.7	68.0	94.1	78.4	49.1	0.4
FD (June-July)	58.6	92.4	90.0	72.3	100.0	92.7	96.1	76.6	0.7
FD (July-August)	92.2	90.6	90.0	56.8	100.0	92.1	96.0	82.8	0.8
FD (August-Sept)	92.5	94.1	96.2	90.8	100.0	96.1	96.0	88.7	0.9
FD (Sept-Oct)	96.3	94.1	96.7	77.0	100.0	96.1	100.0	89.5	0.9
FD (June-July-August)	92.5	100.0	100.0	99.3	100.0	92.6	100.0	96.0	0.9
FD (July-August-Sept)	96.4	96.3	100.0	98.7	100.0	94.6	100.0	96.0	0.9
Pauli (July-August)	57.2	96.5	57.5	89.9	92.0	100.0	100.0	79.4	0.7
Pauli (August-Sept)	46.9	91.8	75.5	69.4	96.0	100.0	100.0	76.4	0.7
Pauli (Sept-Oct)	58.2	90.0	77.7	65.5	90.0	91.2	100.0	68.3	0.6
Pauli (July-August-Sept)	76.4	98.8	90.6	91.2	100.0	100.0	100.0	90.1	0.9
FD+Pauli (July-August)	26.7	44.7	71.3	24.5	94.0	67.2	86.2	49.6	0.4
FD+Pauli (July-August-Sept)	63.0	74.1	92.6	58.1	96.0	69.1	96.0	70.6	0.6
Pauli+HO (July-August)	27.0	69.4	77.7	57.4	96.0	94.6	100.0	67.9	0.6
Pauli+HO (July-August-Sept)	25.7	69.4	69.6	66.9	94.0	45.6	100.0	51.9	0.4
H-A and FD+Pauli (July-August)	91.2	83.5	76.6	71.6	92.0	100.0	100.0	90.1	0.9
H-A and Pauli+HO (July-August)	26.1	92.9	71.3	66.2	96.0	100.0	100.0	66.3	0.6
H-A and RVI (July-August)	55.1	69.4	66.0	59.5	94.0	100.0	100.0	73.7	0.7

IV. CONCLUSION

Temporal variation SAR Polarimetric parameters and associated scattering mechanism were studied for major 'Kharif crops' and associated land cover in North western region of India. Radar Vegetation Index and Polarimetric Decomposition theorems were found to be useful in the identifying and discriminating the given land use based on its scattering mechanisms, not only for an overall temporal change detection, but also feature level changes in scattering behavior over time.

Radar Vegetation Index retrieved from C- band quadpol data was found to be very useful not only in demarcating the aerial extent of effective agricultural areas (RVI >0.45) from the non-agricultural ones (0- 0.45), but also classifying the poor vegetation areas (0.2 to 0.4), moderately cultivated (0.45 to 0.8), and fully grown agricultural patches (RVI> 0.8), based on the difference in RVI ranges. Furthermore, how the RVI values for each feature class changes, based on the internal and structural changes (growth cycle) was clearly observable in the case of the major Kharif crops. Cotton, Paddy and Gwar could be well discriminated based on change in RVI values with respect to their individual growth cycles. Cotton was found to have overall high RVI values over the entire growth cycle ranging from 0.56 to 0.65 from June to October respectively, followed by Gwar and Paddy. Clear trend of decrease in RVI values (0.52 to 0.29) for fallow areas was observed from June to September, showing the replacement of fallow with Kharif crops. Nonagricultural classes like urban and water body had similar RVI values throughout the season, being less than 0.2.

The Freeman Durden Decomposition and Pauli decomposition helped in clearly understanding the dominant scattering properties like double/ even bounce, surface/ odd bounce, and volume/ dihedral bounce of various feature classes like urban, water and crop sub-types respectively. Heterogeneous targets like crop subtypes, fallow areas and water body were better discriminated over time and space using Freeman Durden Decomposition, while homogenous features like urban settlements in comparison to former were clearly demarcated using Pauli Decomposition. From both decompositions, maximum scattering intensity was seen in September month, during which the crops were fully matured (high biomass content).

These scattering components, further helped in improving the classification accuracy of the given study area in combination with the quadpol backscatter bands. Temporally, in all cases, highest classification accuracy was obtained for three date data of July, August and September months. Highest Classification accuracy was obtained in case of Freeman Durden Decomposition (95%), followed by Pauli Decomposition (90%) and RVI parameter (49%). Freeman Durden Decomposition was found to have 5% higher classification accuracy

than Pauli Decomposition, and about 45% higher than RVI.

The results obtained in this study show the importance of polarimetric parameters and decomposition techniques for classification of crops and land uses.

V. REFERENCES

[1] Ainsworth, T.L, Kelly, J.P. and Lee, J.-S., "Classification comparisons between dual-pol, compact polarimetric and quad-pol SAR imagery," ISPRS Journal of Photogrammetry and Remote Sensing, vol. 64, pp. 464-471, 2009.

[2] Cloude, S.R. and E. Pottier, "A review of target decomposition theorems in radar polarimetry", IEEE Trans. GRS, vol. 34(2), pp. 498-518, Mar. 1996.

[3] Cloude S.R. and E. Pottier, "An Entropy-Based Classification Scheme for Land Applications of Polarimetric SAR", IEEE Trans GRS, vol. 35(1), pp. 68-78, 1997.

[4] Dipanwita Haldar, Anup Das, Manoj Yadav, Ramesh S. Hooda, Shiv Mohan, and Manab Chakraborty. "Analysis of Temporal Polarization Phase Difference for Major Crops in India". Progress in Electromagnetic Research. (PIER B), Vol.57, pg. 299-309, 2014.

[5] Durden, S.L., Van Zyl, J.J. and Zebker, H.A., "Modeling and observation of the radar polarization signature of forested areas", IEEE Transactions on Geoscience and Remote Sensing, 27 (3), 290-301, 1989.

[6] Freeman, A. and Durden, S.L. (1992) "A three-component scattering model to describe polarimetric SAR data", Proc. SPIE Conference on Radar Polarimetry, pp. 213-224, San Diego, CA.

[7] Freeman, A. and Durden, S.L. (1998) "A three-component scattering model for polarimetric SAR data", IEEE Transactions on Geoscience and Remote Sensing, vol. 36, no. 3, pp. 963-973.

[8] Imhoff, M., Story, M., Vermillion C., Khan, F. and Polcyn, F., "Forest canopy characterization and vegetation penetration assessment with space-borne radar," IEEE Trans. Geosci. Remote Sensing, vol. GE-24, pp. 535-542, 1986.

[9] Kim, Y. and Van Zyl, J., "Comparison of forest parameter estimation techniques using SAR data," Proc. IGARSS 2001, vol. 3, pp. 1395- 1397, 9-13 July 2001.

[10] Saroj Maity, C. Patnaik, Jai Singh Parihar, Sushma Panigrahy, and K. Ashoka Reddy, "Study of Physical Phenomena of Vegetation Using Polarimetric Scattering indices and Entropy", IEEE Journal of Selected Topics in Applied Earth Observations and Remote Sensing, Vol. 4, No. 2, June 2011.

[11] Shiv Mohan, Anup Das, Dipanwita Haldar and Saroj Maity, "Monitoring and Retrieval of Vegetation Parameter using Multi-frequency Polarimetric SAR data", Asia Pacific Conference on Synthetic Aperture Radar, Seoul, Korea, September, 26-30, 2011.

[12] Varsha Turkar, Rinki Deo, Y.S.Rao, Shiv Mohan, Anup Das, "Classification accuracy of multi-frequency and multi-polarization SAR images for various land covers", IEEE Journal of Applied Earth Observation and Remote Sensing, Vol. 5, No. 3, pp. 936-942, 2012.

[13] Wolfgang-Martin Boerner, Jong-Sen Lee , Dale L. Schuler, Thomas L. Ainsworth, Irena Hajnsek, Kostas P. Papathanassiou, Ernst Lüneburg, "A Review of Polarimetric SAR Algorithms and Their Applications", Journal of Photogrammetry and Remote Sensing Volume 9, No. 3, September 2004, pp. 31-80.

[14] F. Ling , Z. Li, E. Chen, Q. Wang, "Comparison of ALOS PALSAR RVI and Landsat TM NDVI for Forest Area Mapping", 978-1-4244-2732-1/09, 2009 IEEE.